

## Singular Solutions of a Boussinesq System for Water Waves

Jerry L. Bona<sup>1,\*</sup> and Min Chen<sup>2</sup>

<sup>1</sup> Department of Mathematics, Statistics and Computer Science, University of Illinois at Chicago, Chicago IL 60607, USA.

<sup>2</sup> Department of Mathematics, Purdue University, West Lafayette IN 47907, USA.

Received August 5, 2016; Accepted September 1, 2016

---

**Abstract.** Studied here is the Boussinesq system

$$\begin{aligned}\eta_t + u_x + (\eta u)_x + au_{xxx} - b\eta_{xxt} &= 0, \\ u_t + \eta_x + \frac{1}{2}(u^2)_x + c\eta_{xxx} - du_{xxt} &= 0,\end{aligned}$$

of partial differential equations. This system has been used in theory and practice as a model for small-amplitude, long-crested water waves. The issue addressed is whether or not the initial-value problem for this system of equations is globally well posed. The investigation proceeds by way of numerical simulations using a computer code based on a semi-implicit, pseudo-spectral code. It turns out that larger amplitudes or velocities do seem to lead to singularity formation in finite time, indicating that the problem is not globally well posed.

**AMS subject classifications:** 35Q02, 35E02, 76B02, 65B02

**Key words:** Boussinesq systems, global wellposedness, singular solutions, Fourier spectral method, nonlinear water wave.

---

## 1 Introduction

A class of multi-dimensional Boussinesq systems of the form

$$\begin{aligned}\eta_t + \nabla \cdot \mathbf{v} + \nabla \cdot \eta \mathbf{v} + a\Delta \nabla \cdot \mathbf{v} - b\Delta \eta_t &= 0, \\ \mathbf{v}_t + \nabla \eta + \frac{1}{2}\nabla |\mathbf{v}|^2 + c\Delta \nabla \eta - d\Delta \mathbf{v}_t &= 0,\end{aligned}\tag{1.1}$$

---

\*Corresponding author. *Email addresses:* jbona@uic.edu (J. Bona), chen45@purdue.edu (M. Chen)

was put forward in [6] as models for the propagation of small amplitude, long wavelength surface water waves. Here,  $\eta = \eta(x, y, t)$  describes the height of the free surface, relative to its rest position, above the point  $(x, y, 0)$  on the bottom and the vector  $v = v(x, y, \theta, t)$  has components  $(u, w)$  representing the horizontal velocity field at height  $\theta$  above the same point. The gradient, divergence and Laplacian are all taken with respect to the horizontal spatial variables  $(x, y)$ . The overlying assumptions leading to such models are that the ratio  $\alpha$  of the waveheight to the undisturbed depth be small, the ratio  $\beta$  of the undisturbed depth to a typical wavelength be small, but that the quotient  $\alpha/\beta^2$  be of order one. As written in (1.1), the horizontal coordinates  $x$  and  $y$  are measured in wavelengths whereas the vertical coordinate  $z$  is measured in depths. A consequence of the latter fact is that  $\theta \in [0, 1]$ . The constants  $a, b, c, d$  have the form

$$a = \left(\frac{\theta^2}{2} - \frac{1}{6}\right)\lambda, \quad b = \left(\frac{\theta^2}{2} - \frac{1}{6}\right)(1-\lambda), \quad c = \frac{1-\theta^2}{2}\nu, \quad d = \frac{1-\theta^2}{2}(1-\nu), \quad (1.2)$$

where  $\lambda$  and  $\nu$  are modeling parameters which may take any real value without disturbing the formal level of approximation inherent in such models. Details of the derivation and scaling being used may be found in [6, 7, 12].

The system (1.1) of three, coupled, nonlinear evolution equations allows for propagation in all directions. The long-crested regime is where most of the motion takes place in the  $x$ -direction, say, with little or no variation in the  $y$ -direction. In this case, the model simplifies. The second component  $w$  of the horizontal velocity  $v$  is zero, derivatives with respect to  $y$  vanish and the third equation is satisfied identically. The system then reduces to

$$\begin{aligned} \eta_t + u_x + (\eta u)_x + a u_{xxx} - b \eta_{xxt} &= 0, \\ u_t + \eta_x + \frac{1}{2}(u^2)_x + c \eta_{xxx} - d u_{xxt} &= 0, \end{aligned} \quad (1.3)$$

where  $a, b, c$  and  $d$  are as above and subscripts connote partial differentiation.

Mathematical theory for various of both the one- and two-dimensional versions of this class of Boussinesq systems appears in [1, 3, 5-7, 12, 21-25], for example. In particular, combining the results in [12], the existence theory for the model equations mentioned above and similar results for the full water-wave problem in [2], one sees that these systems are indeed approximations of the full, inviscid, water wave problem with rigorous error estimates that validate the formal asymptotics that go into their derivation.

The results in the papers about the Boussinesq models reveal that some of the  $abcd$ -systems are well posed, at least locally in time. These are the candidates for use in practical situations. However, for almost all of these systems, there is little information available as to whether or not they are globally well posed, even for small data. (The exceptions are what is termed the original Boussinesq system, see [25] and [3], which is globally well posed for arbitrary-sized, localized, smooth initial data and the Bona-Smith system [10] which is globally well posed for order-one initial data.

In this paper, we will concentrate on one special member of the one-dimensional system (1.3), namely

$$\begin{aligned} \eta_t + u_x + (u\eta)_x - \frac{1}{6}\eta_{xxt} &= 0, \\ u_t + \eta_x + uu_x - \frac{1}{6}u_{xxt} &= 0, \end{aligned} \tag{1.4}$$

which obtains by taking  $\theta^2 = 2/3$  and  $\lambda = \nu = 0$ . This particular member of the class (1.3) has been used in a number of contexts (see e.g. [5], [13] ) and it has many helpful mathematical properties, *viz.*

- The linearized system is globally well posed in  $L^p$  and in  $W_p^k$  for  $1 \leq p \leq \infty$  and  $k = 0, 1, 2, \dots$ .
- Global well-posedness in time for the nonlinear problem is proved in [1] under the condition that there is an  $\alpha > 0$  such that the solution satisfies

$$1 + \eta(x, t) \geq \alpha \quad \text{for all } t \geq 0. \tag{1.5}$$

Note that this is an imperfect result because it is based on an assumption about the solution  $\eta$  which is not known to be verified from conditions on the initial data. In physical terms, the condition (1.5) simply means that the bed does not run dry at any time, or what is the same, the free surface never touches the impermeable bottom.

- It has the invariant functionals

$$\begin{aligned} H(\eta, u) &= \frac{1}{2} \int_{-\infty}^{\infty} u^2(1 + \eta) + \eta^2 dx, \\ I(\eta, u) &= \int_{-\infty}^{\infty} u\eta + \frac{1}{6}\eta_x u_x dx, \\ I_u &= \int_{-\infty}^{\infty} u dx \quad \text{and} \quad I_\eta = \int_{-\infty}^{\infty} \eta dx. \end{aligned}$$

Moreover, there is a Hamiltonian structure based on  $H$  and  $I$ , namely

$$\partial_t \nabla_{(\eta, u)} I(\eta, u) + \partial_x \nabla_{(\eta, u)} H(\eta, u) = 0,$$

where  $\nabla_{(\eta, u)}$  is the Euler derivative. As pointed out in [7], none of these invariant functionals are composed only of positive terms, so they do not on their own provide the *a priori* information one needs to conclude global existence of solutions of initial-value problems. However, they are useful in helping assess the accuracy of a numerical scheme for approximating solutions of the system.

- The system has solitary-wave solutions (single hump, traveling-wave solutions) [20], cnoidal-wave solutions [15], standing waves [17], doubly periodic solutions [18,19] and multi-pulsed solutions [16].
- High accuracy, unconditionally stable numerical schemes for the system (1.4) are straightforward to construct. Numerical investigation of the stability and interaction of various special solutions may be found in [5].
- The system has the exact solution

$$\begin{aligned} u_{\pm}(x,t) &= \pm \frac{15}{2} \operatorname{sech}^2 \left( \frac{3}{\sqrt{10}} \left( x \mp \frac{5}{2}t \right) \right), \\ \eta_{\pm}(x,t) &= \frac{15}{2} \operatorname{sech}^2 \left( \frac{3}{\sqrt{10}} \left( x \mp \frac{5}{2}t \right) \right) - \frac{45}{4} \operatorname{sech}^4 \left( \frac{3}{\sqrt{10}} \left( x \mp \frac{5}{2}t \right) \right), \end{aligned} \quad (1.6)$$

which are also helpful for checking the accuracy of numerical schemes.

- The system (1.4) can be posed on the half-line or on a bounded interval with a minimum of auxiliary boundary conditions. This is especially helpful when attempting to use the model in a laboratory or field setting, as in [9]. The pure initial-value problem is seldom of practical applicability.

Despite these very satisfactory results, the fundamental issue of determining conditions on the initial data that ensure the solution exists for all time still remains. The present contribution aims to cast light on this issue. The investigation is carried out computationally, using an accurate computer code in an exploratory mode. It will transpire that there are initial data that appear to blow up in finite time and others that support globally defined solutions. The simulations provide clues as to what conditions are needed to ensure global solutions exist. These are discussed in Sections 3 and 4, which are preceded by a short section providing accuracy checks for the numerical scheme.

## 2 Accuracy and convergence of the numerical scheme

The scheme used to simulate the system (1.3) is a semi-implicit, Fourier-pseudo-spectral method. Solutions on the entire real line  $\mathbb{R}$  are approximated by finite Fourier series, which works well provided they remain suitably localized (see [4] and [14] for theory concerning this type of approximation). More precisely, first invert the operator  $I - \frac{1}{6}\partial_x^2$  subject to periodic boundary conditions to obtain the system

$$V_t = L(V) + N(V)$$

where  $V = (\eta, u)$ ,  $L$  is the linear part of the equation and  $N$  is the nonlinear operator. The operator  $L$  is computed spectrally while the nonlinear part of  $N$  is computed in the original variables and the non-local operator  $(I - \frac{1}{6}\partial_x^2)^{-1}$  is computed on the result spectrally.

Table 1: Error of  $L_\infty$  and  $L_2$  norm of  $\eta$  and  $u$ , with respect to  $\Delta t$ .

$\Delta t$	6.4e-03	3.2e-03	1.6e-03	8.0e-04	4.0e-04	2.0e-04	1.0e-04
$\ \eta\ _\infty$ error	7.6e-04	2.7e-06	5.8e-05	1.5e-05	3.6e-06	9.0e-07	2.3e-07
$\ u\ _\infty$ error	1.1e-03	1.9e-04	7.5e-05	1.9e-05	4.7e-06	1.2e-06	3.0e-07
$\ \eta\ _2$ error	4.4e-05	1.1e-05	2.8e-06	7.1e-07	1.8e-07	4.5e-08	1.1e-08
$\ u\ _2$ error	1.2e-04	3.0e-05	7.5e-06	1.9e-06	4.7e-07	1.2e-07	3.0e-08

The time stepping is implemented semi-implicitly via the scheme

$$\frac{u^{n+1} - u^{n-1}}{2\Delta t} = \frac{L(u^{n+1}) + L(u^{n-1})}{2} + N(u^n)$$

where  $u^k = u^k(x)$  is the Fourier series approximation of the vector  $V(x,t)$  at the time  $t = k\Delta t, k = 0, 1, 2, \dots$ . This scheme should be second order in time and have spectral convergence in space, facts that can be rigorously proved, but we pass over this point here. It was observed that the scheme is stable, again a point that can be proved rigorously, but is not considered in detail here.

The numerical method was checked for correct coding using the exact traveling-wave solutions displayed in (1). The spatial discretization error was ascertained by using a step size that is so small that the temporal discretization does not contribute to the error much beyond about machine accuracy. We started the computation with initial data as in (1) specified on the spatial interval  $[-10, 10]$  and applied periodic boundary conditions at the ends of the spatial interval. We compared the exact solution with the calculated solution at  $T = 1$ . With  $\Delta t = 0.0001$ , the error associated with the approximation of  $(\eta, u)$ , in the  $L_\infty$  norm, is  $(2.3 \times 10^{-7}, 3.0 \times 10^{-7})$  as soon as  $\Delta x$  is smaller than about 0.1, which is to say, the number of modes taken in the spectral approximation is more than about 200. The convergence was seen to be spectral in nature, as expected.

Similar calculations are performed to investigate the time discretization error. For  $\Delta x$  fixed at 0.02, i.e. 1000 modes, the error in the  $L_\infty$  norm and  $L_2$  norm of  $(\eta, u)$  with respect to  $\Delta t$  are shown in Table 1. Note that the numerical study of the temporal error indicates clearly that the algorithm is indeed second order in time.

### 3 Interaction of exact traveling waves

Once one is sure of the code, it is an interesting first foray to ask what happens if two of these exact traveling-wave solutions are allowed to interact. To this end, take for initial data a sum

$$(\eta_+(x - x_+, 0), u_+(x - x_+, 0)) + (\eta_-(x - x_-, 0), u_-(x - x_-, 0)) \tag{3.1}$$

of a widely separated right-moving and left-moving wave. The spatial domain was chosen to be  $[-14, 14]$  and  $x_\pm = \pm 7$ . Notice that this special initial data has  $\eta(x, 0)$  an even

function of  $x$  whereas  $u(x,0)$  is an odd function. For such smooth, localized initial data, the local well-posedness theory insures that there are solutions defined on some positive time interval that lie in  $H^k(\mathbb{R})$  for any  $k=1,2,\dots$ .

Remark first that if the  $L^\infty$ -norm of either  $\eta$  or  $u$  remains bounded on a time interval  $[0,T]$ , then the other does as well. For consider the elementary energy identity

$$\frac{d}{dt} \int_{-\infty}^{\infty} \left( u^2 + \eta^2 + \frac{1}{6}u_x^2 + \frac{1}{6}\eta_x^2 \right) dx = 2 \int_{-\infty}^{\infty} \eta_x u \eta dx$$

obtained by multiplying the first equation by  $\eta$ , the second by  $u$ , summing the two results and then integrating over  $\mathbb{R}$  and integrating by parts. If either  $\eta$  or  $u$  is uniformly bounded on  $\mathbb{R} \times [0,T]$ , then a Gronwall-type argument applied to this identity reveals immediately that the  $H^1(\mathbb{R})$ -norm of both  $\eta$  and  $u$  are bounded on the same interval. (Indeed, it suffices for one of  $\eta$  and  $u$  to be bounded in  $L^2(\mathbb{R})$ -norm on  $[0,T]$  to draw this conclusion.)

Second, observe that the system (1.4) is invariant under the transformation  $u \rightarrow -u$  and  $x \rightarrow -x$ . Thus if  $(\eta(x,t), u(x,t))$  is a solution, so is  $(\eta(-x,t), -u(-x,t))$ . As the initial data posited above has  $\eta(x,0)$  even and  $u(x,0)$  odd, it itself is invariant under this transformation. The uniqueness of solutions to the initial-value problem thus implies that  $\eta(x,t)$  will be an even function and  $u(x,t)$  an odd function of  $x$  as long as they exist. Hence, if there is to be a single-point blow-up of the solution emanating from (3.1), it must occur at  $x=0$ . Indeed, this is exactly what appears to happen. The interaction of these two traveling waves apparently leads to the  $L^\infty$ -norm of both  $\eta$  and  $u$  becoming infinite at  $x=0$  at a fixed, finite time. Here is a sketch of the evidence in favor of this conclusion.

**Solution Plots** The evolution of the solution is plotted in Fig. 1 for  $t=0$  (the initial data) and  $t=1.5, 3.25$  and  $t=4.75$ . The value  $\eta(0,t)$  approaches  $-\infty$  as  $t$  approaches  $t_0$  and the velocity variable  $u(x,t)$  appears also to be blowing up, becoming unboundedly positive on the set  $\{(x,t) : -\nu < x < 0, t < t_0\}$  and unboundedly negative on the set  $\{(x,t) : 0 < x < \nu, t < t_0\}$  for any  $\nu > 0$ .

The computation is terminated when the absolute value of  $\eta$  at any spatial point exceeds  $10^{10}$ .

**Local Similarity Structure** Blow up for nonlinear, dispersive wave equations often shows a similarity structure, at least near the blow-up point. An early appreciation of this point may be found in the work of Weinstein [26] on the generalized KdV equation. See also [8] for analysis and graphics depicting local similarity structure for these equations.

The possibility of (local) similarity blow-up was tested in our case by monitoring the blow-up rates of various norms of the blowing up solution. In more detail, if a function  $f(x,t)$  is in the form

$$f(x,t) = \frac{1}{t^r} F\left(\frac{x}{t^q}\right) \tag{3.2}$$

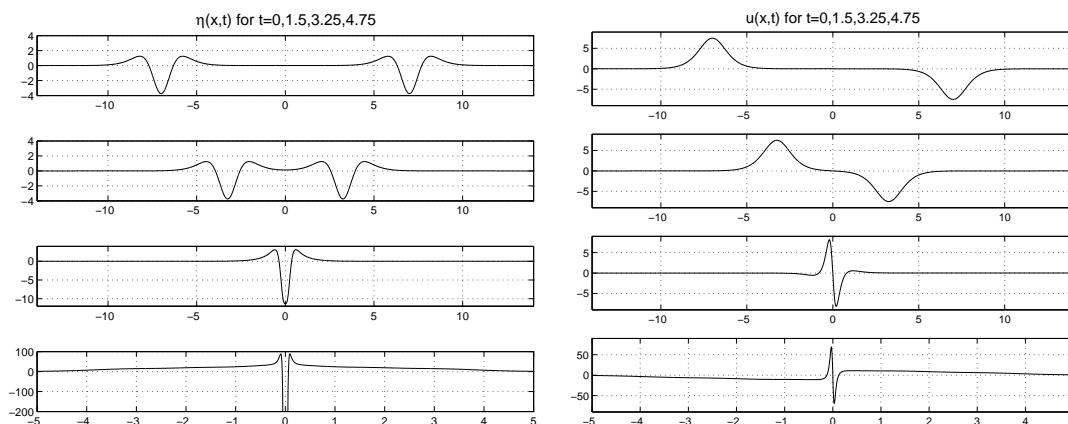


Figure 1: The head-on collision of exact traveling-wave solutions of the BBM-BBM system.

where  $F$  is a function in  $L_p$  for  $1 \leq p \leq \infty$ , then it has

$$\|f\|_{L_\infty} = O(t^{-r_\infty})$$

and

$$\|f\|_{L_p} = \frac{1}{t^{r_\infty}} t^{q/p} \left( \int F^p \left( \frac{x}{t^q} \right) \frac{1}{t^q} dx \right)^{1/p} = O(t^{q/p - r_\infty}) = O(t^{-r_p}).$$

Thus, the quantity

$$r_p = r_\infty - \frac{q}{p}$$

is the blow-up rate for the  $L_p$ -norm when it is positive, which will certainly be true if  $r_\infty > 0$  and  $p$  is large enough. In particular,  $r_2 = r_\infty - \frac{1}{2}q$ . Thus, a knowledge of  $r_\infty$  and  $r_2$  allows determination of the value of  $q$  and thereby, in principle, the blow-up rate in  $L_p$ -norm for any other value of  $p$  from the formulas

$$q = 2(r_\infty - r_2), \quad r_p = r_\infty - \frac{2(r_\infty - r_2)}{p}. \tag{3.3}$$

The conjecture (3.2) is now examined in the light of (3.3). The computation is carried out with 28000 Fourier modes and a time step  $\Delta t = \frac{1}{10000}$ . The value of  $t_0$  is approximated as the time when  $\|\eta\|_{L_\infty}$  reaches  $10^{10}$ . In this case, it has the value  $t_0 = 5.1725$ . The log-log plot of  $\|\eta\|_{L_\infty}, \|\eta\|_{L_2}, \|u\|_{L_\infty}, \|u\|_{L_2}$  with respect to  $t_0 - t$  is shown in Fig. 2 for the time interval  $4.5 < t < 5.1$ . Notice that the solution seems to be well settled into a similarity structure in this time range. Using a least square approximation, the blowup rate for the  $L^p$ -norms for  $p = 1, 2, \dots, 10$  are computed and plotted in Fig. 3. Using the data obtained for the  $L^\infty$  and  $L^2$ -norms of  $\eta$  and  $u$ , which are 2.49 and 2.21 for  $\eta$  and 1.21 and 0.95 for  $u$ , respectively, the values of  $r_p$  are calculated using (3.3) and plotted in Figure 3. The  $L_p$ -norms of  $\eta$  are very well predicted by (3.3), but the  $L_p$ -norms of  $u$  show some discrepancy

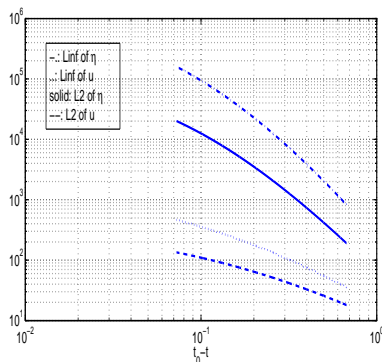


Figure 2: Plot of the log of various  $L^p$ -norms with respect to  $\log(t_0 - t)$  for  $4.5 < t < 5.1$ .

for lower values of  $p$ . The  $L^1$ -norms are not as well matched as the  $L^p$ -norms for  $p > 2$ , probably because  $I_\eta = \int_{\mathbb{R}} \eta dx$  is constant in time, as is  $I_u = \int_{\mathbb{R}} u dx$ . From these data, one is tempted to conjecture that near the blow-up point  $(x, t) = (0, t_0)$ , the solution has the similarity structure

$$\eta(x, t) = \frac{1}{(t - t_0)^{2.5}} N\left(\frac{x}{(t - t_0)^{0.5}}\right), \quad u(x, t) = \frac{1}{(t - t_0)^{1.25}} U\left(\frac{x}{(t - t_0)^{0.5}}\right)$$

as  $x \rightarrow 0$  and  $t \rightarrow t_0$ , for suitable shape functions  $N$  and  $U$ . Fig. 4 plots the solution at two times close to the blow-up point.

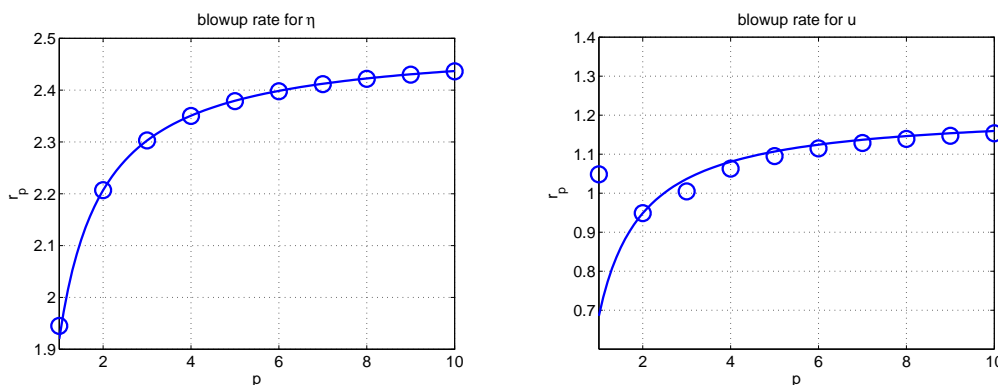


Figure 3: Comparison between predicted rates of blowup using the similarity hypothesis with numerically computed rates.

It deserves remark that if the blow up has a similarity structure, this is probably only local around the blow-up point  $(0, t_0)$ . Deviation from pure similarity blow up can be

discerned by computing the function

$$-\frac{\max_x \eta(x,t)}{\min_x \eta(x,t)}.$$

If a pure similarity was to obtain globally, this should approach a constant as  $t \rightarrow t_0^-$ . Graph 5 shows it to be a linear function of  $t$  for  $t$  near  $t_0$ , thereby indicating that the hypothesis (3) does not hold globally over the entire interval. Note also that the rates posited in (3) could easily be off by logarithms, as these might be invisible at the numerical level.

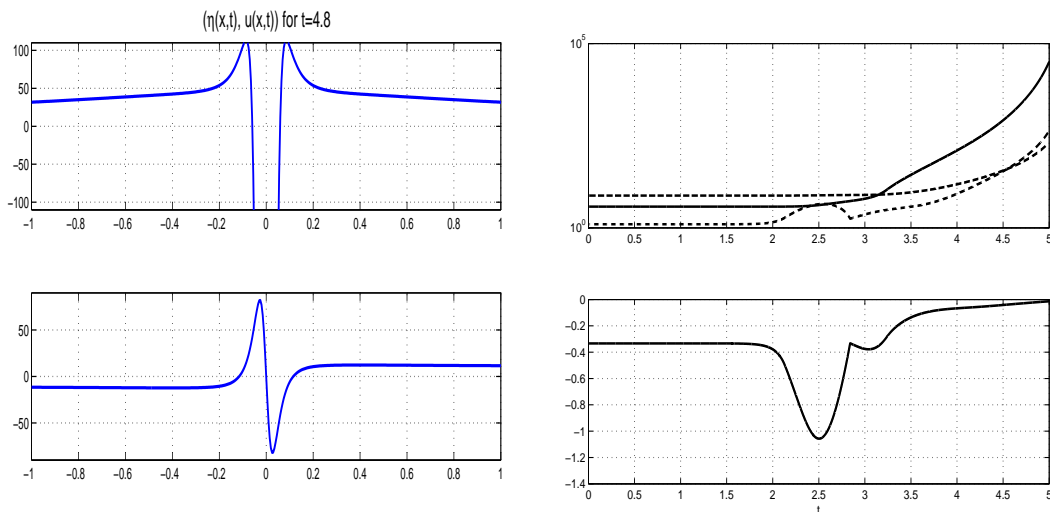


Figure 4: Closer look near the blow up point and the maximum.

### 4 Initial profiles constructed from Gaussians and their derivatives

The tentative conclusion derived from the information in the last section is that there are solutions emanating from certain initial data that blow up in finite time. On the other hand, the exact traveling-wave solutions displayed in (1) are obviously globally defined. In this section, we delve a little more deeply into this dichotomy, with particular attention given to the transition from globally defined to blowing up solutions.

In the simulations reported below, we will be using  $N = 200 \times L$  Fourier components, where  $L$  is the width of spatial interval, and  $\Delta t$  will be set to  $1/2000$  unless otherwise noted. The choice  $200 * \Delta t = \frac{1}{10}$  insures that when blowup occurs, an accurate approximation of the blowup time  $t_0$  is forthcoming. The  $L$  is always chosen large enough that no significant energy reaches and wraps around the boundary. Outcomes of the simulations were checked by halving the temporal mesh size, doubling the number of Fourier

components and increasing the width of the interval. The solution curves were virtually indistinguishable in all cases.

A solution was declared to be 'global' if it failed to blow up (*i.e.*  $\eta$  stays below  $10^{10}$  in absolute value) on the time interval  $[0, T_{end}]$  where  $T_{end}$  was here taken to be 40. This criterion was tested with longer runs and found to be satisfactory for the sort of initial data described below. Indeed, we observed that blow-up of solutions corresponding to these initial data, if it is to occur, will typically happen very rapidly. (Though, obviously, the interaction of traveling waves that was the subject of Section 3 could be postponed as long as one likes by simply increasing the separation in the right- and left-going wave at time  $t=0$ .)

We began the investigation with Gaussian profiles of various amplitudes for both  $\eta$  and  $u$ . As already noted, the Boussinesq system (1.4) is invariant under the transformation  $u \rightarrow -u$  and  $x \rightarrow -x$ . Hence the sign of  $u$  plays no role in whether or not the solution is global. Thus, if  $\eta_0$  is symmetric in  $x$ , as Gaussians are, and if  $(\eta_0, u_0)$  is initial data leading to a globally defined solution, then  $(\eta_0, -u_0)$  does also. However, for  $\eta$ , positive and negative values can be distinguished, as will be seen presently. The first tests were performed with both  $\eta(x,0)$  and  $u(x,0)$  having Gaussian profiles of the form  $\eta_0 e^{-x^2}$  and  $u_0 e^{-x^2}$ , respectively. Solutions in this case seem to be globally defined for waves of elevation, where we allowed amplitudes  $\eta_0$  and  $u_0$  in the entire range  $(0, 5)$ , but mixed for waves of depression.

Guided by the situation obtaining in Section 3, where the initial velocity was of both signs, we tested initial data of the form

$$\eta(x,0) = a e^{-x^2}, \quad u(x,0) = b x e^{-x^2} \quad (4.1)$$

with varying values of  $a$  and  $b$ . Notice in this case that  $\|\eta(x,0)\|_{L^\infty} = |a|$  and  $\|u(x,0)\|_{L^\infty} = \frac{|b|}{\sqrt{2}} \approx 0.707|b|$ . Fig. 5 gives an indication of what happens to the solution when a range of values of  $a$  and  $b$  are chosen. Provisional conclusions deriving from this set of experiments are as follows:

- The size of the wave,  $\|\eta(\cdot,0)\|_{L^\infty}$ , alone is not an indicator of blow up. For example, with  $a = -2, b = 0$ , the solution blows up, but with  $a = -2, b = 4$ , the solution remains bounded.
- The set of values  $(a,b)$  which generate global solutions appears to be a connected set in the plane. This is indicated in the 'blow-up map' in Fig. 5. The  $x$ 's connote values of  $(a,b)$  where the solution blows up and the circles are values where the solution appears global.
- Waves of depression (initial data featuring negative values of  $\eta$ ) are more likely to blow up.
- Values of  $a > -1$  correspond to physical situations where the bottom has no dry spots initially. That is to say the total initial height  $h(x,0) = 1 + \eta(x,0)$  of the wave is positive. In this case, provided that  $b$  is small, it seems that a global solution exists.

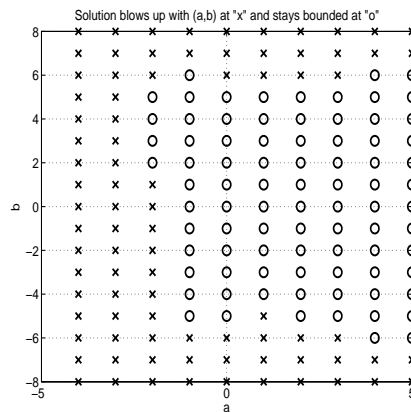


Figure 5: Blowup map for values of the parameters  $a$  and  $b$ .

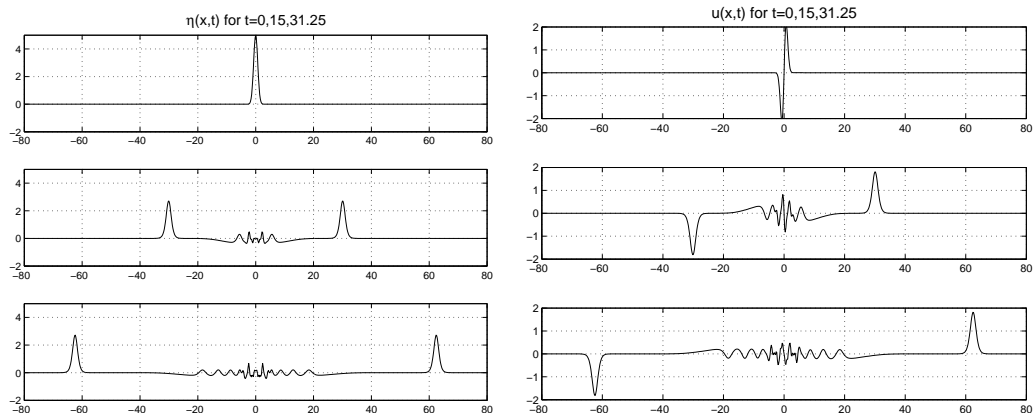


Figure 6:  $a=5, b=5$ . The initial wave of elevation resolves into a pair of solitary waves propagating in different directions, each trailing a dispersive tail.

- The collision of left- and right-moving waves can cause large variations in  $u$  near the collision point and this in turn can lead to blow up.

Several representative cases are now described in detail. The first one has data of the form shown in (4.1) with  $a = b = 5$ , a wave of elevation. As the initial horizontal velocity  $u(x,0)$  is negative for  $x < 0$  and positive for  $x > 0$ , one expects the solution to break into right- and left-propagating waves. This is indeed the case and after while, these two wavetrains cease to interact. They are led by a solitary wave and followed by a dispersive tail. Snapshots of the solution at three time are plotted in Fig. 6; the solution seems to exist globally in time. A further argument in favor of this conclusion can be made based on the comparison results between the system (1.4) and the unidirectional *BBM* model

$$\eta_t + \eta_x + \frac{3}{2}\eta\eta_x - \frac{1}{6}\eta_{xxt} = 0$$

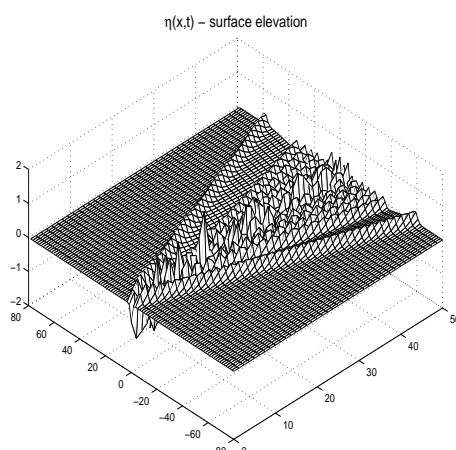


Figure 7:  $a = -0.5, b = 5$ , starting from a wave of depression, a solitary waves develop propagating at the front in each direction, trailing complex dispersive tails.

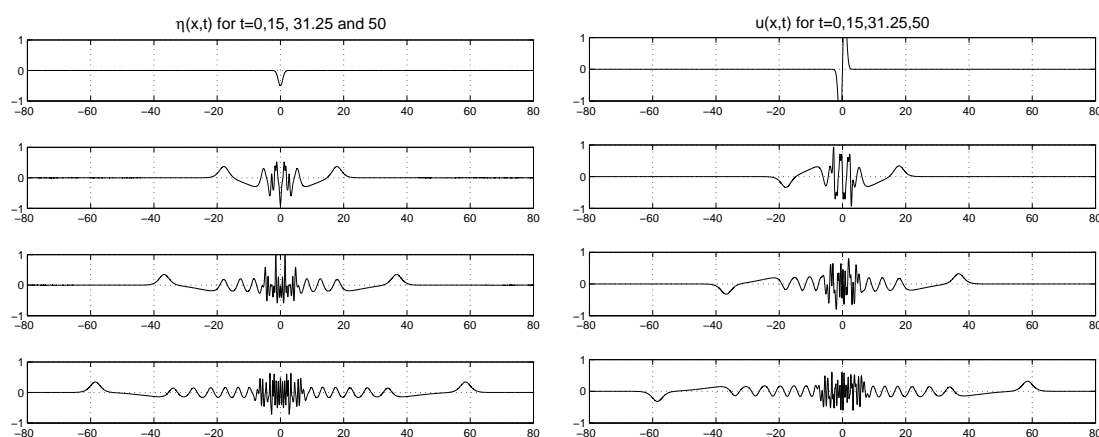


Figure 8:  $a = -0.5, b = 5$ , snapshots of the waves at  $t = 0, 15, 31.25$  and  $50$ .

developed in [1], but this point is not pursued here.

The next case begins life as a wave of depression with  $a = -0.5, b = 5$ . The blow-up map in Fig. 5 reveals that for  $b$  small, the solution exists globally in time. However, as  $b$  is increased, the solution ceases to be global. The evolution of the solution when  $b = 5$  is shown in a space-time plot in Fig. 7 while Fig. 8 shows more detailed spatial plots at various times. The norms of the solution  $(\eta, u)$  and the conserved quantities  $I_\eta, I_u$  and  $H(\eta, u)$  are computed and plotted as a function of time in Fig. 9. The degree to which the invariants  $I_\eta, I_u$  and  $H(\eta, u)$  remain constant is an indication of the accuracy of our numerical scheme.

The amplitude of the velocity is now turned up, so  $a = -0.5$  and  $b = 8$ . The solution emanating from this initial configuration blows up near  $T_{end} = 14.7$ . The solution structure

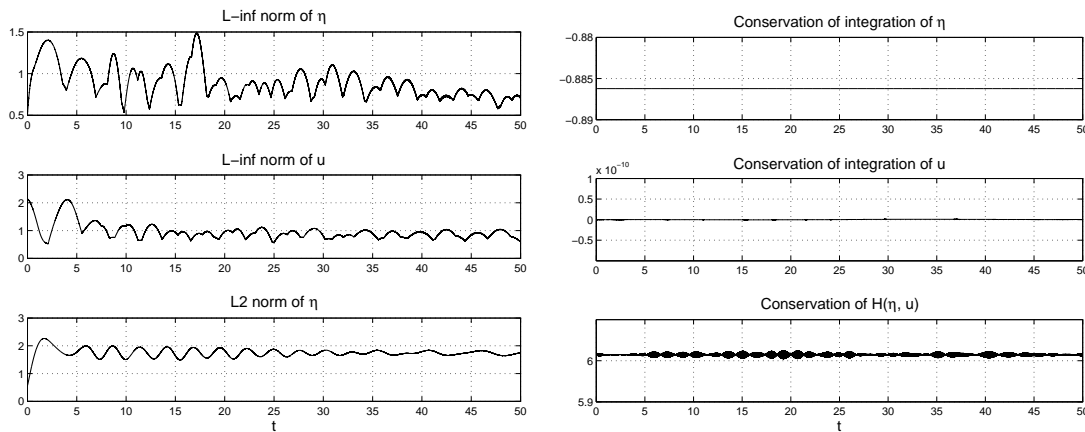


Figure 9:  $a = -0.5, b = 5$ , the norms of the solution and the conserved quantities as functions of time.

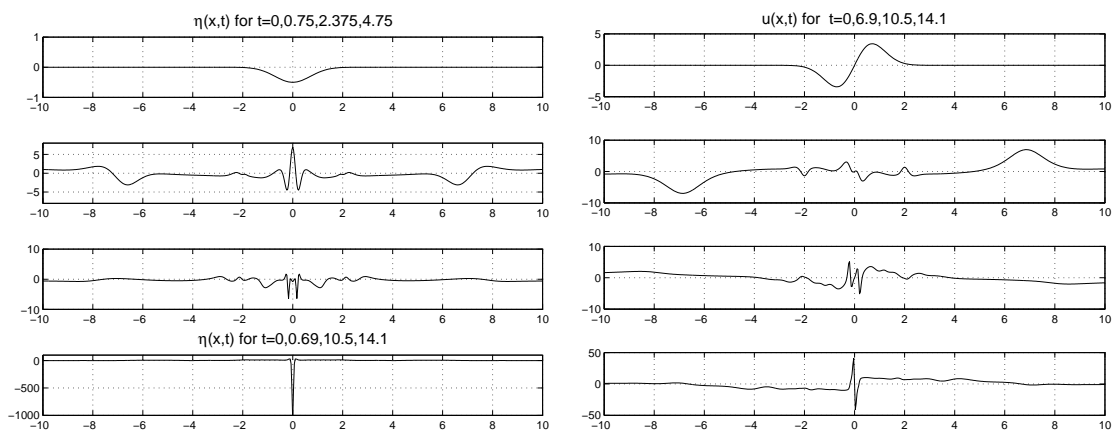


Figure 10:  $a = -0.5, b = 8$ , snapshots of the solution.

is plotted at a sequence of times in Fig. 10. Notice that the solution blows up at the center  $x = 0$ , in accord with the symmetry of the initial data.

A closer look near the blow-up time is plotted in Fig. 11. There is a wave group traveling in each direction. At the middle, the solution blows up, or rather, “blows down” to be more precise.

For this case, an even smaller value,  $\Delta t = 0.0002$  is used and the number of modes is raised to  $600 \times 28$  to be sure of keeping the solution under control in the face of very large gradients. It is worth noting that the condition  $1 + \eta(x, 0) \geq \alpha > 0$  which is the case when  $a = -.5$  does not ensure that  $1 + \eta(x, t) > 0$  for all  $t > 0$ , nor does it imply the solution remains bounded for all  $t > 0$ .

Another case exhibiting blowup is plotted in Fig. 12. Here, the parameters are  $a = -5$  and  $b = 5$ . A common structure near the blowup point seems to appear here also. This is consistent with the idea that there is a family of similarity structures which emerge, at

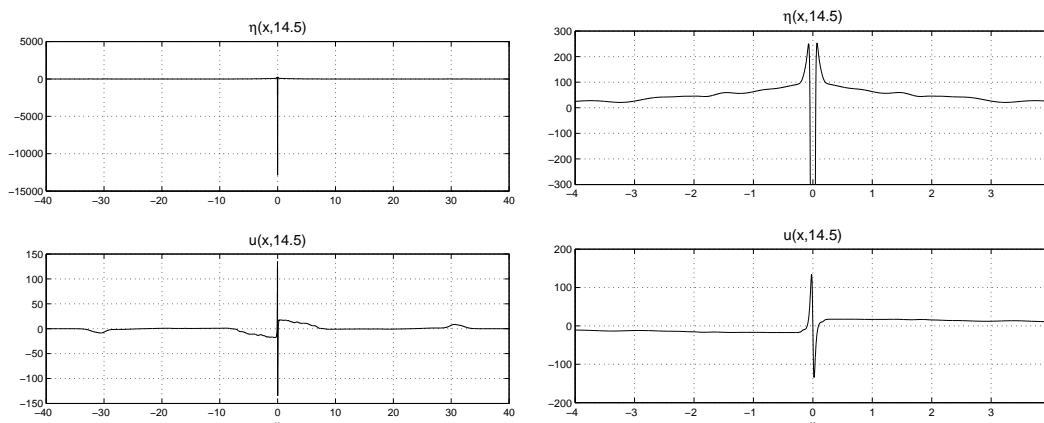


Figure 11:  $a = -0.5, b = 8$ , solutions near the blowup time; a closer look.

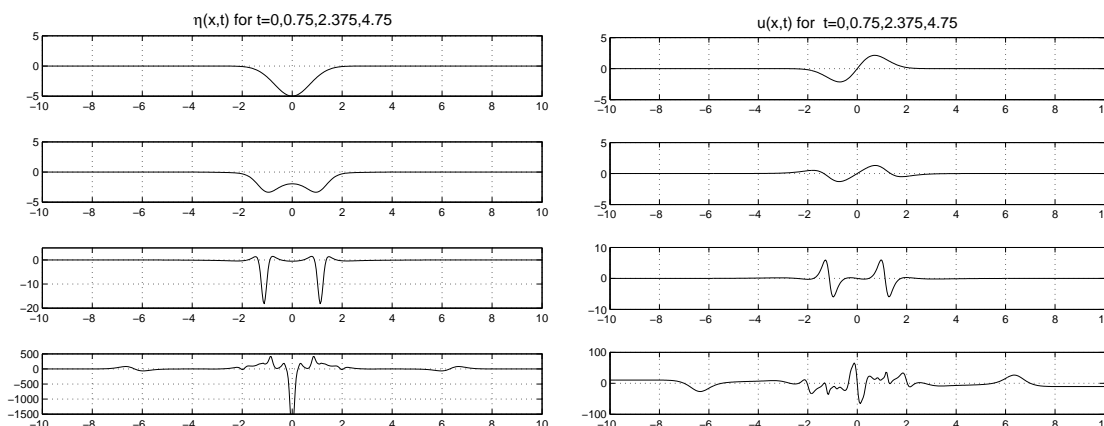


Figure 12: Snapshots of waves with  $a = -5, b = 5$ .

least near the blowup point. However, it is clear from the evolution of the profiles that the similarity structure does not extend globally in space. For while  $\eta$  concentrates near  $x = 0$ , the two positive wings are seen to spread, which is not consistent with (3.2). The same kind of local similarity structure was observed for the blowup in the generalized Korteweg-de Vries equation (see Fig. 7 in [8]), but it was proved in [11] that the similarity cannot extend to the entire solution (see also Fig. 10 in [8]).

### Acknowledgments

The genesis of this project took occurred while both authors were visiting the Tsinghua Sanya International Mathematics Forum. Part of the writing was done while JB was an NCTS visiting professor at Taiwan National University. The authors are grateful for the fine working conditions provided during these visits. MC would like to thank Simons

Foundation for its support under grant number 198275.

## References

- [1] A. A. Alazman, J. P. Albert, J. L. Bona, M. Chen, J. Wu, Comparisons between the BBM equation and a Boussinesq system, *Adv. Differential Equations*, **11**(2)(2006),121–166.
- [2] B. Alvarez-Samaniego, D. Lannes, Large time existence for 3d water-waves and asymptotics, *Inventiones*, **171**(3)(2008), 485–541.
- [3] C. J. Amick, Regularity and uniqueness of solutions to the Boussinesq system of equations, *J. Diff. Eq.*, **54**(2)(1984), 231–247.
- [4] J. L. Bona, Convergence of periodic wave trains in the limit of large wavelength, *Appl. Sci. Res.*, **37**(1981), 21–30.
- [5] J. L. Bona, M. Chen, A Boussinesq system for two-way propagation of nonlinear dispersive waves, *Physica D*, **116**(1998),191–224.
- [6] J. L. Bona, M. Chen, J.-C. Saut, Boussinesq equations and other systems for small-amplitude long waves in nonlinear dispersive media I: Derivation and the linear theory, *J. Nonlinear Sci.*, **12**(4)(2002), 283–318.
- [7] J. L. Bona, M. Chen, J.-C. Saut, Boussinesq equations and other systems for small-amplitude long waves in nonlinear dispersive media II: Nonlinear theory, *Nonlinearity*, **17**(3)(2004), 925–952.
- [8] J. L. Bona, V. A. Dougalis, O. A. Karakashian, W. R. McKinney, Conservative, high-order numerical schemes for the generalized Korteweg-de Vries equation, *Philos. Trans. Royal Soc. London, Ser. A*, **351**(1695)(1995), 107–164.
- [9] J. L. Bona, W. G. Pritchard, L. R. Scott, An evaluation of a model equation for water waves, *Philos. Trans. Royal Soc. London, Ser. A*, **302**(1981), 457–510.
- [10] J. L. Bona, R. Smith, A model for the two-way propagation of water waves in a channel, *Math. Proc. Cambridge Philos. Soc.*, **79**(1976), 167–182.
- [11] J. L. Bona, F. B. Weissler, Similarity solutions of the generalized Korteweg-de Vries equation, *Math. Proc. Cambridge Phil. Soc.*, **127**(2)(1999), 323–351.
- [12] Jerry L. Bona, Thierry Colin, David Lannes, Long wave approximations for water waves, *Arch. Ration. Mech. Anal.*, **178**(3)(2005), 373–410.
- [13] R. C. Cascaval, A boussinesq model for pressure and flow velocity waves in arterial segments, *Math. Computers Simulation*, **82**(6)(2012), 1047–1055.
- [14] H. Chen, Long-period limit of nonlinear, dispersive waves: the BBM-equation, *Differential Integral Eqns*, **19**(2006), 463–480.
- [15] H. Chen, M. Chen, N. V. Nguyen, Cnoidal wave solutions to boussinesq systems, *Nonlinearity*, **20**(6/1)(2007), 1443–1461.
- [16] M. Chen, Solitary-wave and multi-pulsed traveling-wave solutions of Boussinesq systems, *Appl. Anal.*, **75**(1-2)(2000), 213–240.
- [17] M. Chen, G. Iooss, Standing waves for a two-way model system for water waves, *European Journal of Mechanics B/Fluids*, **24**(1)(2005), 113–124.
- [18] M. Chen, G. Iooss, Periodic Wave Patterns of two-dimensional Boussinesq systems, *European Journal of Mechanics B/Fluids*, **25**(2006), 393–405.
- [19] M. Chen, G. Iooss, Asymmetrical Periodic Wave Patterns of two-dimensional Boussinesq systems, *Physica D*, **237**(2008), 1539–1552.
- [20] M. Chen, N. V. Nguyen, S. M. Sun, Existence of traveling-wave solutions to boussinesq systems, *Differential and Integral Equations*, **24**(9/10)(2011), 895–908.

- [21] V. Dougalis, D. Mitsotakis, J.-C. Saut, On some boussinesq systems in two space dimensions: theory and numerical analysis, *ESIAM: M2AM*, **41**(5)(2007), 825–854.
- [22] F. Linares, D. Pilod, J.-C. Saut, Well-posedness of strongly dispersive two-dimensional surface waves boussinesq systems, *SIAM J. Math. Anal.*, **44**(6)(2012), 4195–4221.
- [23] M. Ming, J.-C. Saut, P. Zhang, Long-time existence of solutions to boussinesq systems, *SIAM J. Math. Anal.*, **44**(6)(2012), 4078–4100.
- [24] J.-C. Saut, L Xu, The cauchy problem on large time for surface waves boussinesq systems, *J. Math. Pures Appliq.*, **97**(2012), 635–662.
- [25] M. E. Schonbek, Existence of solutions for the Boussinesq system of equations, *J. Diff. Eq.*, **42**(3)(1981), 325–352.
- [26] Michael I. Weinstein, On the structure and formation of singularities in solutions to nonlinear dispersive evolution equations, *Comm. Partial Differential Equations*, **11**(5)(1986), 545–565.